LncRNA MALAT1 regulates growth of carcinoma of the lung through modulating miR-338-3p/PYCR2 axis

Yang Geng[1], Pengfei Chen[1], Lei Zhang[1], Xiaojun Li[1], Chao Song[1], Xueting Wei[2], Huiyuan Gong[1,*]

[1] Department of Thoracic Surgery, The First Affiliated Hospital of Bengbu Medical College, Bengbu, Anhui 233004, China

[2] Department of Molecular Diagnostic Center, The First Affiliated Hospital of Bengbu Medical College, Bengbu, Anhui 233004, China

ARTICLE INFO

ABSTRACT

The progression of several cancers, including lung cancer, has been linked to long non-coding RNAs (lncRNAs) (LC). The current research concentrated on elucidating the effects of MALAT1 on the course of LC and investigating potential pathways. The qPCR and in situ hybridization (ISH) assays were used to measure MALAT1 expression in LC tissues. Additionally, the overall survival (OS), a percentage of LC patients with various MALAT1 levels was examined. Additionally, it was determined whether MALAT1 was expressed in LC cells through qPCR analysis. LC cells' proliferation, apoptosis, and metastasis were all examined concerning MALAT1 utilizing the following techniques: EdU, CCK-8, western blot and flow cytometry. This study predicted and verified the correlation between MALAT1, microRNA (miR)-338-3p as well as pyrroline-5-carboxylate reductase 2 using bioinformatics and dual-luciferase reporters (PYCR2). On the activity and function of MALAT1/miR-338-3p/PYCR2 in LC cell activities, more study was conducted. The amount of MALAT1 was raised in LC tissues and cells. Low OS was seen in patients with elevated MALAT1 expression. By inhibiting MALAT1, LC cells saw decreased migration, invasion, and proliferation as well as an increase in apoptosis. Additionally, PYCR2 appeared as an objective of miR-338-3p, while MALAT1 was a target of miR-338-3p. Additionally, the over-expression of miR-338-3p had effects that were comparable to those of MALAT1 down-regulation. The function of miR-338-3p inhibitor on the functional activities of LC cells co-transfected with sh-MALAT1 was partially recovered by PYCR2 inhibition. MALAT1/miR-338-3p/PYCR2 maybe the novel target for LC therapy.

Introduction

Lung cancer (LC) is one of the most prevalent malignant tumors in the entire globe, with a five-year survival rate of fewer than 18% (1). Further to that, LC is quite prevalent, seriously jeopardizing human life and health (2). The two distinct pathogenic types of LC are small-cell lung cancer as well as non-small-cell lung cancer (3). There are still no sensitive and precise early diagnosis techniques, despite some advancements in diagnosing and treating LC (4). Although low-dose spiral CT for LC screening can somewhat increase the detection rate of LC, it also has several very clear limits. The psychological burden on patients is further increased by its high false positive rate (5). The evaluation and analysis of clinicopathological sections serve as a "gold standard" for the high-precision diagnosis of LC as well as its varieties. Numerous variables, including the sampling procedure, tumor location, reader expertise, etc., have an impact on sampling and analysis (6). Along with the very few available treatment options for LC, a major issue is that this condition is highly susceptible to medication resistance (7). Consequently, the goal of current LC research is to identify useful molecular indicators for LC diagnosis and prospective gene therapy targets.

MicroRNAs (miRNAs) have received the majority of attention in the last ten years from researchers studying the regulatory mechanisms of non-coding RNA (8). Long non-coding RNAs (lncRNAs) have been discovered in multiple studies to play a crucial role in the formation and metastasis of malignant tumor cells. However, artificially inhibiting lncRNA expression levels can effectively suppress the tumor cells' malignant behavior, providing us with a novel approach to cancer therapy (9). LncRNAs are long, linear RNA molecules that cannot code for proteins (10). They have a length of more than 200 nt. Currently, it is understood that lncRNAs can participate in a variety of molecular processes that control LC advancement, indirectly controlling cell malignancy such as malignant transformation, drug sensitivity, proliferation, metastasis, and other processes (11). For instance, LC tissues and cells have increased levels of NNT-AS1. NNT-AS1 knockdown reduces LC cell growth and invasion while promoting apoptosis. In LC tissues, there is a rise in TUC338 expression (12). TUC338 expressions are not connected with age or gender, but rather with the patient's overall survival, tumor size, and lymph node metastasis (13). Similarly observed in LC, in high-grade LC tissues as well as aggressive cancer cells in particular, is the up-regulation of differentiation antagonizing noncoding RNA (DANCR). While DANCR silencing has the opposite consequences, ectopic DANCR expression promotes LC cell proliferation and colony formation (14). These findings suggest that lncRNAs have a major impact on the emergence of LC.

On human chromosome 11q13, there is a long nonco-

ding RNA (lncRNA) known as MALAT1, which is involved in several malignancies (15). MALAT1 is originally described as an LC prognostic marker (16). MALAT1 promotes migration, colony formation, chemoresistance, and other cancerous characteristics in LC cells, according to later research, which points to its carcinogenesis (17). The varied and intricate nature of MALAT1 action mechanisms, however, calls for additional investigation using a variety of methods. Hence, the purpose of this study was to explore possible approaches and ascertain if MALAT1 had a physiological role in the progression and metastasis of LC.

Materials and Methods

Clinic samples

The First Affiliated Hospital of Bengbu Medical College provided the LC tissues as well as the matching tissues for collection. All patients were untreated before sample collection. Besides, this study was authorized by the Ethics Committee after each participant provided written informed permission for participation.

MALAT1 bioinformatics analysis in LC

From TCGA, gene expression data and associated clinical details for LC were retrieved. Analysis of MALAT1 expression in terms of overall survival (OS).

Cell culture and transfection

DMEM provided by Thermo Fisher Scientific (Waltham, MA, USA) with 10% FBS provided by Thermo Fisher Scientific was used to cultivate BEAS-2B cells as well as LC cells (A549, HCC827, H1299, and H1650) at 37°C and 5% CO_2.

Short hairpin (shRNA)-expressing lentivirus vectors were created from Genechem to target MALAT1 or pyrroline-5-carboxylate reductase 2 (PYCR2), as well as shRNA negative controls (sh-NC), NC mimic/microRNA (miR)-338-3p mimic, and NC inhibitor/miR-338-3p inhibitor (Shanghai, China). Moreover, every aforementioned plasmid was separately transfected into LC cells using Lipotransfectamine 6000 provided by Thermo Fisher Scientific (Waltham, MA, USA) for 48 hours as directed.

CCK-8 assay

Different groups' transfected LC cells (2×10^3) were planted onto 96-well plates. CCK-8 kit provided by Sigma (St. Louis, MO, USA) was conducted after being cultu-

red for 48 hours. Using a spectrophotometer provided by Molecular Devices (Eugene, OR, USA), absorbance (OD) (450 nm) was discovered.

EdU assay

Various groups' transfected LC cells were treated with the EdU reaction solution for 30 minutes. LC cells were then trypsinized, fixed with formaldehyde, and washed in PBS containing 1% BSA. Triton X-100 was adopted to permeabilize cells, PBS was used to rinse them, and fluorescence microscopy (Leica Microsystems, Wetzlar, Germany) was utilized to inspect the cells.

Flow cytometry analysis

Different groups' transfected LC cells were collected and then washed. Next, the cells were treated for 15 minutes with 10 μL of Annexin V-FITC as well as 10 μL of PI. To identify apoptotic cells, a flow cytometer provided by BD Biosciences (Franklin Lakes, NJ, USA) was used.

Wound-healing assay

In 6-well plates, transfected LC cells (5×10^5/well) from several groups were arranged. A wound was scraped once cells had 80% confluence. Light microscopy (Nikon, Tokyo, Japan) (200×) was employed to photograph the cell pictures at 0 and 48 hours

Transwell assay

Transfected LC cells were grown in the top compartment of the migration assay using the basal media. 600 μL of medium with 10% FBS were given to the lower chambers. Cells were immobilized with methanol after 48 hours, then stained with 0.1% crystal violet, and counted while being seen under a microscope (Leica, Wetzlar, Germany). The top membrane was pre-coated with Matrigel provided by Franklin Lakes (NJ, USA) for the invasion experiment. The alternative techniques resembled cell migration.

qPCR analysis

All RNA extracted from LC tissues as well as cells were then adopted to make cDNA by the RNeasy plus micro kit as the raw material for qPCR utilizing the Step One System provided by Life Technologies Corp (Gaithersburg, MD, USA). The sequences of all primers were generated utilizing Primer Premier software 4.0 provided by Premier (Canada), as indicated in Table 1. The $2^{-\Delta\Delta CT}$ technique normalized β-actin and U6.

Table 1. Primer sequences.

Gene name	Primer sequences
MALAT1	F: 5'-GGTAACGATGGTGTCGAGGTC-3'
	R: 5'-CCAGCATTACAGTTCTTGAACATG-3'
miR-338-3p	F: 5'-ATCCAGTGCGTGTCGTGG-3'
	R: 5'-TGCTTCCAGC ATCAGTGAT-3'
PYCR2	F: 5'-CCTAGCGTTACTTCCGGTCC-3'
	R: 5'-AGCCATGAATGCCTTCTCCA-3'
β-actin	F: 5'-TCCCATCACCATCTTCCAGG-3'
	R:5'-GATGACCCTTTTGGCTCCC-3'
U6	F: 5'-CTCGCTTCGGCAGCACA-3'
	R: 5'-AACGCTTCACGAATTTGCGT-3'

Western blot assay

Bidicinchoninic acid (BCA) kit provided by Beyotime Biotechnology (Shanghai, China) was adopted to assay the protein that was isolated from LC cells. Using SDS-PAGE (10%), the protein was then extracted and converted onto PVDF membranes provided by Millipore (Billerica, MA, USA). Next, primary antibodies were applied to the membranes overnight at 4°C using 5% skimmed milk. The antibodies are as follows: anti-Bax (1: 2, 000, bs20337R, Bioss, Woburn, MA, USA), anti-Bcl-2 (1: 2, 000, bs20352R, Bioss, Woburn, MA, USA), anti-Cleaved caspase-3 (1: 2, 000, bs33199M, Bioss, Woburn, MA, USA), anti-MMP-2 (1: 2, 000, bs20705R, Bioss, Woburn, MA, USA), anti-MMP-9 (1: 2, 000, bs7095R, Bioss, Woburn, MA, USA), anti-PYCR2 (1: 2, 000, bs19690R, Bioss, Woburn, MA, USA) and anti-β-actin (1: 2, 000, bs0061R, Bioss, Woburn, MA, USA), with β-actin which was treated as the endogenous control. In the next step, membranes were further incubated with a secondary antibody (1: 2,000, b-0311P-HRP, Bioss, Woburn, MA, USA) for an additional hour. Subsequently, protein blots were viewed using ECL (Millipore, Billerica, MA, USA).

***In situ* hybridization (ISH)**

The embedded sections underwent a five-minute incubation with HCL at room temperature followed by three PBS washes. Then polyformaldehyde was incubated for a further 10 minutes after Protease K (15 µg/mL) had been incubated continuing for 20 minutes. Then, kept at room temperature, the acetic anhydride and triethanolamine solution was incubated for 10 minutes. The probe was applied to the sections after being diluted by the hybridization solution and sealed overnight at 37°C. Afterward, it was denatured at 85°C for 5 min. Correspondingly, sections were exposed to BCIP/NBT for 48 hours in the dark after being treated with anti-digoxin I antibody (1: 1,000) overnight at 4°C and photographed utilizing an inverted microscope (Nikon, Tokyo, Japan).

Luciferase reporter assay

In this study, MALAT1 or PYCR2 WT/MUT were sub-cloned to produce pmirGLO-MALAT1 or pmirGLO-PYCR2 WT/MUT for co-transfection with NC mimic or miR-338-3p mimic in LC cells. The functionality and reaction of luciferase were examined 48 hours after co-transfection (Promega, Madison, WI, USA).

Statistical analysis

The mean ± standard deviation (SD) of the data obtained from three repetitions is displayed. GraphPad Prism 8.0 software provided by GraphPad Software (Inc., La Jolla, CA, USA). The t-test utilized to help distinguish between the two groups, the single-factor ANOVA used to analyze the groups, and the Tukey post-test all show that the difference is statistically significant ($P < 0.05$).

Results

MALAT1 is inversely correlated with prognosis and up-regulated in LC tissues as well as cells

First, qPCR and ISH were employed to assess MALAT1 expressions in LC tissues in order to look into the potential function of MALAT1 in LC advancement. Figures 1A and 1B show that MALAT1 levels were elevated in LC
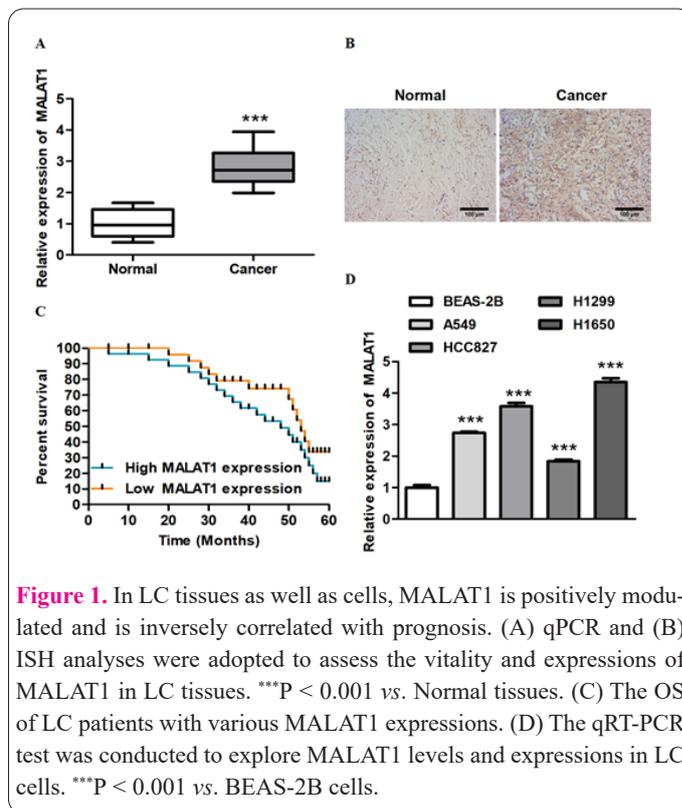

Figure 1. In LC tissues as well as cells, MALAT1 is positively modulated and is inversely correlated with prognosis. (A) qPCR and (B) ISH analyses were adopted to assess the vitality and expressions of MALAT1 in LC tissues. ***P < 0.001 *vs*. Normal tissues. (C) The OS of LC patients with various MALAT1 expressions. (D) The qRT-PCR test was conducted to explore MALAT1 levels and expressions in LC cells. ***P < 0.001 *vs*. BEAS-2B cells.

tissues. Additionally, Kaplan-Meier analysis revealed that Figure 1C's LC patients with low MALAT1 expressions had longer OS than those with high MALAT1 expressions. Moreover, a qPCR assay was used to find MALAT1 expressions in LC cells. According to Figure 1D's data, LC cells have strong MALAT1 expression (especially in HCC827 and H1650 cells). These findings showed that MALAT1 could be crucial to the development of LC since it was significantly expressed in LC tissues as well as cells.

MALAT1 down-regulation prevents LC cells from proliferating and causes them to undergo apoptosis

Sh-NC or sh-MALAT1 were functionally transfected into LC cells, and Figure 2A demonstrates the efficacy of the transfection. CCK-8 and EdU were introduced to assert and examine the impact of MALAT1 on the viability of LC cells. Figures 2B and 2C demonstrate how MALAT1 down-regulation prevented LC cells from proliferating. Similarly, flow cytometry analysis was employed to evaluate MALAT1's impacts on the LC cells' apoptosis. Figure 2D illustrates how down-regulating MALAT1 caused LC cells to apoptosis. Additionally, the levels of apoptosis-related proteins consisting of Bax, Bcl-2, and cleaved caspase-3 were measured utilizing a western blot assay. As seen in Figure 2E, Bax, as well as Cleaved caspase-3 levels, were up-regulated whereas Bcl-2 levels were down-regulated in LC cells that had been transfected with sh-MALAT1. According to these findings, down-regulation of MALAT1 prevented LC cells from proliferating and caused them to undergo apoptosis.

MALAT1 down-regulation prevents LC cells from migrating and invading

Likewise, a wound-healing experiment was adopted to gauge how MALAT1 affected LC cell motility. MALAT1 down-regulation prevented LC cells from migrating, as illustrated in Figure 3A. Transwell migration and invasion
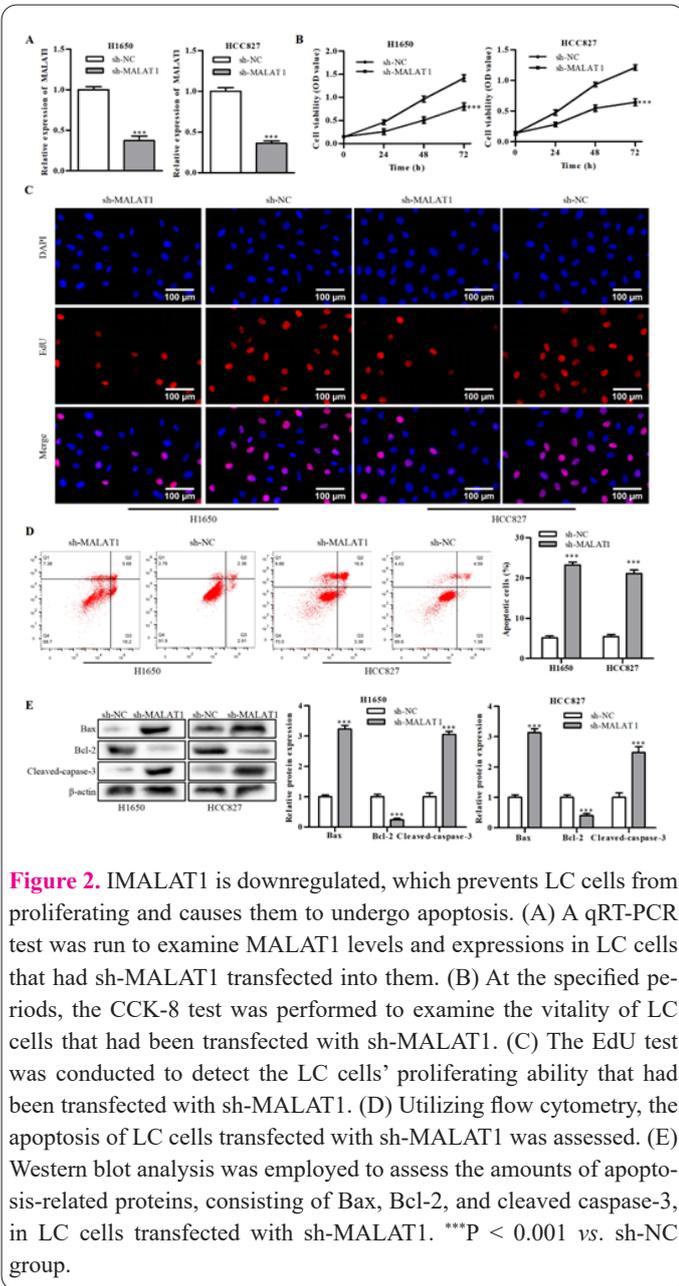
Figure 2. IMALAT1 is downregulated, which prevents LC cells from proliferating and causes them to undergo apoptosis. (A) A qRT-PCR test was run to examine MALAT1 levels and expressions in LC cells that had sh-MALAT1 transfected into them. (B) At the specified periods, the CCK-8 test was performed to examine the vitality of LC cells that had been transfected with sh-MALAT1. (C) The EdU test was conducted to detect the LC cells' proliferating ability that had been transfected with sh-MALAT1. (D) Utilizing flow cytometry, the apoptosis of LC cells transfected with sh-MALAT1 was assessed. (E) Western blot analysis was employed to assess the amounts of apoptosis-related proteins, consisting of Bax, Bcl-2, and cleaved caspase-3, in LC cells transfected with sh-MALAT1. $^{***}P < 0.001$ *vs.* sh-NC group.
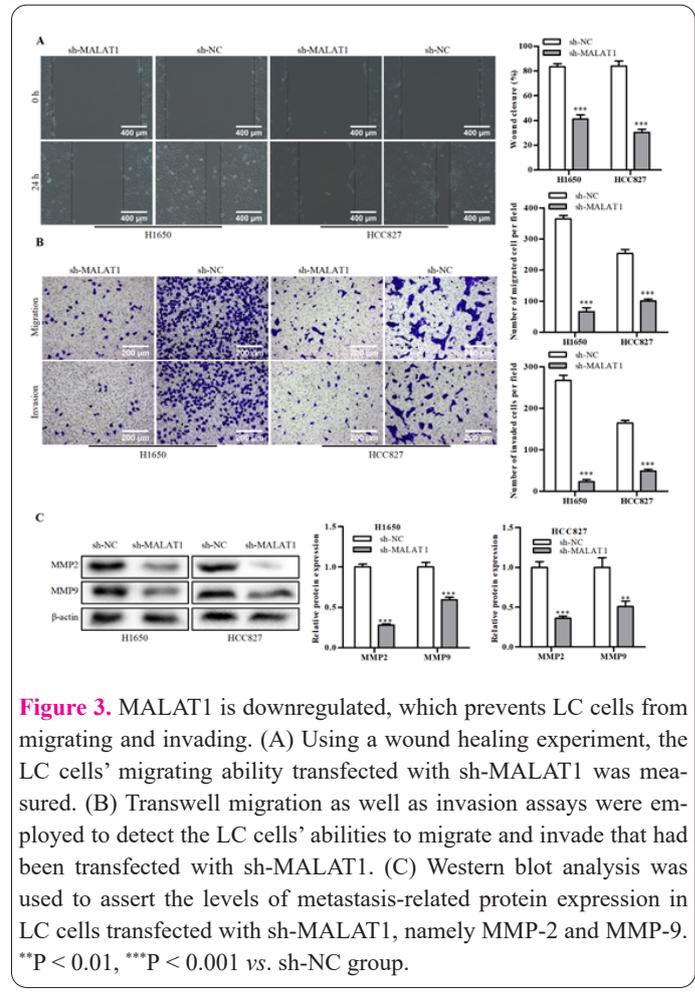
Figure 3. MALAT1 is downregulated, which prevents LC cells from migrating and invading. (A) Using a wound healing experiment, the LC cells' migrating ability transfected with sh-MALAT1 was measured. (B) Transwell migration as well as invasion assays were employed to detect the LC cells' abilities to migrate and invade that had been transfected with sh-MALAT1. (C) Western blot analysis was used to assert the levels of metastasis-related protein expression in LC cells transfected with sh-MALAT1, namely MMP-2 and MMP-9. $^{**}P < 0.01$, $^{***}P < 0.001$ *vs.* sh-NC group.

experiments were further performed. Figure 3B shows that down-regulating MALAT1 prevented LC cells from migrating and invading. Similarly, the quantity of proteins like MMP-2 and MMP-9 that are connected to metastasis was measured using a western blot. Figure 3C showed that MALAT1 down-regulation reduced protein levels of MMP-2 and MMP-9 in LC cells. Thus, these outcomes demonstrated that the down-regulation of MALAT1 hindered the LC cells' abilities to invade and migrate.

Interaction between MALAT1 and miR-338-3p in terms of regulation

Bioinformatics techniques were employed to gather miRNAs that could bind MALAT1 to determine probable MALAT1 pathways. MiR-338-3p was thought to have a MALAT1 target domain, as illustrated in Figure 4A. The dual-luciferase reporter study shown in Figure 4B further supported the link between MALAT1 and miR-338-3p. Additionally, qPCR was used to identify miR-338-3p expression in LC cells transfected with sh-MALAT1. In LC cells that had been transfected with sh-MALAT1, miR-338-3p levels were upregulated, as seen in Figure 4C. Moreover, qPCR investigation revealed the presence

Figure 4. Relationship between MALAT1 and miR-338-3p in terms of regulation. (A) The locations where MALAT1 and miR-338-3p bind. (B) A dual-luciferase reporter experiment was employed to evaluate the relationship between MALAT1 and miR-338-3p. $^{***}P < 0.001$ *vs.* NC mimic group. (C) A qRT-PCR test was adopted to identify the vitality and expressions of miR-338-3p in LC cells transfected with sh-MALAT1. $^{***}P < 0.001$ *vs.* sh-NC group. By using qPCR analysis, the vitality and expressions of MALAT1 in (D) LC tissues as well as (E) cell lines were assessed. $^{***}P < 0.001$ *vs.* Normal tissues or BEAS-2B cells. (F) MALAT1 and miR-338-3p have a negative association in LC tissues.

of miR-338-3p in LC tissues and cells. MiR-338-3p levels were down-regulated in LC tissues and cells, as indicated in Figures 4D and 4E. Furthermore, MALAT1 and miR-

338-3p had an opposite relationship in the LC tissues displayed in Figure 4F. These data indicate that miR-338-3p was a MALAT1 target in LC cells.

MiR-338-3p upregulation prevents LC cells from proliferating and causes them to undergo apoptosis

The efficiency of transfecting LC cells with NC mimic/ miR-338-3p mimic is shown in Figure 5A. CCK-8 and EdU were utilized to determine the functionality of miR-338-3p on the LC cells' ability to proliferate. Figures 5B and 5C demonstrate how the up-regulation of MiR-338-3p stopped LC cells from proliferating. Further, it was investigated how miR-338-3p influenced the apoptosis of LC cells using flow cytometry. Figure 5D shows that the up-regulation of miR-338-3p led to the death of LC cells. Additionally, the quantities of apoptosis-related proteins consisting of Bax, Bcl-2 as well as cleaved caspase-3 were examined through the analysis of western blot. Bax and Cleaved caspase-3 levels were in an up-regulating state whereas Bcl-2 levels were down-regulated in LC cells that

had miR-338-3p mimics transfected into them, which can be seen in Figure 5E. According to these findings, miR-338-3p upregulation prevented LC cells from proliferating and caused them to undergo apoptosis.

MiR-338-3p upregulation prevents LC cells from migrating and invading

Correspondingly, a wound-healing experiment was used to gauge how miR-338-3p affected LC cells' motility. MiR-338-3p mimics reduced LC cell movement, as seen in Figure 6A. Transwell migration and invasion experiments were further performed. Figure 6B confirms that miR-338-3p was upregulated, which prevented LC cells from migrating and invading. To measure the levels of proteins associated with metastasis, such as MMP-2 as well as MMP-9, an assay of the western blot was adopted. In LC cells, miR-338-3p was overexpressed, which caused a decline in the protein levels of MMP-2 as well as MMP-9, as seen in Figure 6C. This analysis shows that miR-338-3p was increased, which stopped the invasion as well as migration of LC cells.

PYCR2 is a miR-338-3p's target

Utilizing bioinformatics methods, it was possible to examine the downstream miR-338-3p targets. The outcomes showed that PYCR2 was a possible miR-338-3p target (Figure 7A). The dual-luciferase reporter analysis depicted in Figure 7B indicated the relationship between miR-338-3p and PYCR2. PYCR2 levels in LC cells that had been transfected with miR-338-3p mimic were discovered using western blot analysis. PYCR2 levels were de-
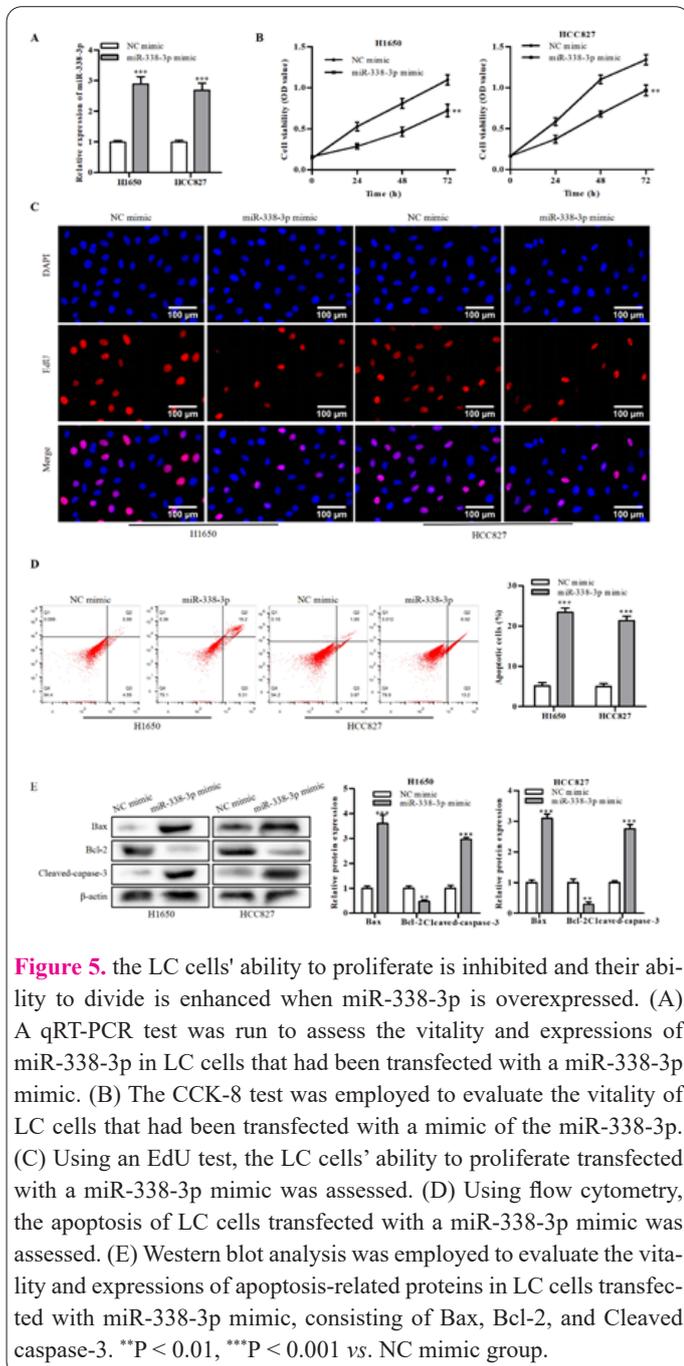

Figure 5. the LC cells' ability to proliferate is inhibited and their ability to divide is enhanced when miR-338-3p is overexpressed. (A) A qRT-PCR test was run to assess the vitality and expressions of miR-338-3p in LC cells that had been transfected with a miR-338-3p mimic. (B) The CCK-8 test was employed to evaluate the vitality of LC cells that had been transfected with a mimic of the miR-338-3p. (C) Using an EdU test, the LC cells' ability to proliferate transfected with a miR-338-3p mimic was assessed. (D) Using flow cytometry, the apoptosis of LC cells transfected with a miR-338-3p mimic was assessed. (E) Western blot analysis was employed to evaluate the vitality and expressions of apoptosis-related proteins in LC cells transfected with miR-338-3p mimic, consisting of Bax, Bcl-2, and Cleaved caspase-3. $^{**}P < 0.01$, $^{***}P < 0.001$ vs. NC mimic group.
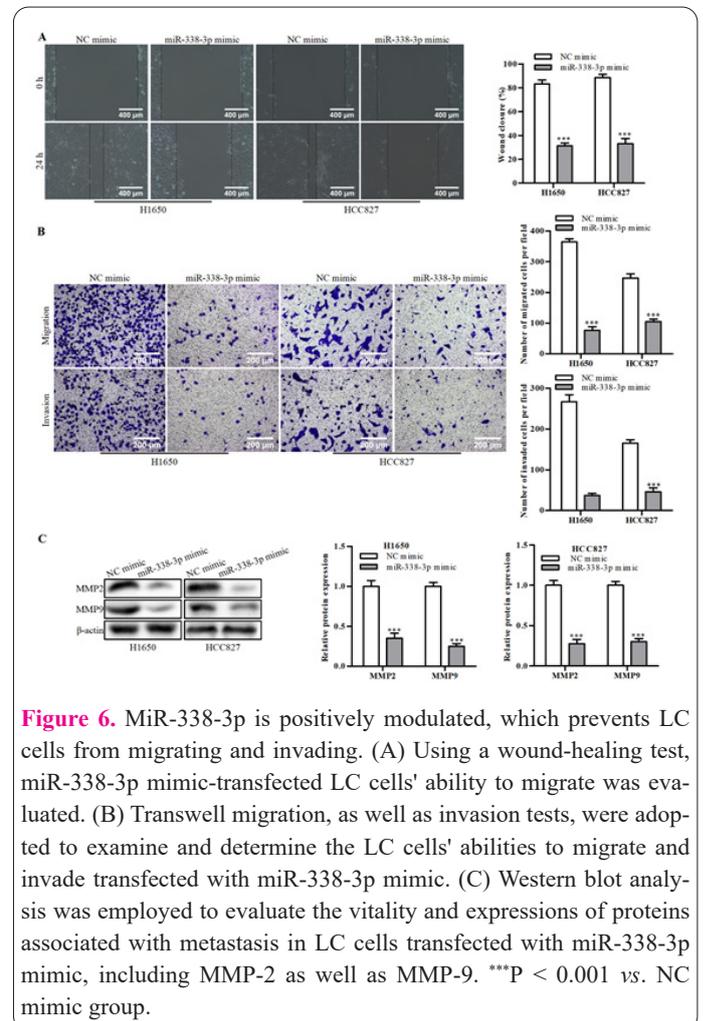

Figure 6. MiR-338-3p is positively modulated, which prevents LC cells from migrating and invading. (A) Using a wound-healing test, miR-338-3p mimic-transfected LC cells' ability to migrate was evaluated. (B) Transwell migration, as well as invasion tests, were adopted to examine and determine the LC cells' abilities to migrate and invade transfected with miR-338-3p mimic. (C) Western blot analysis was employed to evaluate the vitality and expressions of proteins associated with metastasis in LC cells transfected with miR-338-3p mimic, including MMP-2 as well as MMP-9. $^{***}P < 0.001$ vs. NC mimic group.
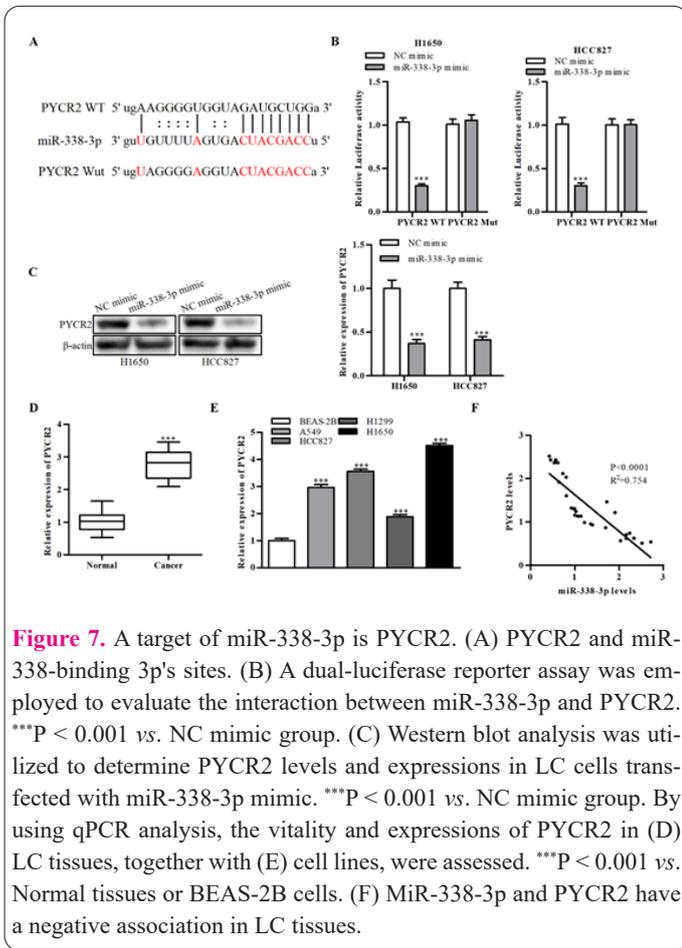
Figure 7. A target of miR-338-3p is PYCR2. (A) PYCR2 and miR-338-binding 3p's sites. (B) A dual-luciferase reporter assay was employed to evaluate the interaction between miR-338-3p and PYCR2. ***P < 0.001 *vs.* NC mimic group. (C) Western blot analysis was utilized to determine PYCR2 levels and expressions in LC cells transfected with miR-338-3p mimic. ***P < 0.001 *vs.* NC mimic group. By using qPCR analysis, the vitality and expressions of PYCR2 in (D) LC tissues, together with (E) cell lines, were assessed. ***P < 0.001 *vs.* Normal tissues or BEAS-2B cells. (F) MiR-338-3p and PYCR2 have a negative association in LC tissues.

Figure 8. MALAT1 controls the miR-338-3p/PYCR2 axis, which controls the metastasis of LC cells. (A) By using a qRT-PCR experiment, the transfection efficiency of LC cells was assessed. **P < 0.01 *vs.* NC inhibitor or sh-NC group. (B) The CCK-8 test was applied at the appropriate periods to identify the vitality of LC cells after transfection. (C) The EdU test was implemented to gauge the LC cells' ability to proliferate following transfection. (D) Flow cytometry analysis was employed to gauge the LC cells' level of apoptosis following transfection. Following transfection, (E) wound-healing as well as (F) transwell assays were applied to examine and determine the LC cells' abilities to migrate and invade. ***P < 0.001 *vs.* sh-NC+NC inhibitor+sh-NC group, ###P < 0.001 *vs.* sh-MALAT1+NC inhibitor+sh-NC group. $$P < 0.01, $$$P < 0.001 *vs.* sh-MALAT1+miR-338-3p inhibitor+sh-NC group.

creased in LC cells that had miR-338-3p mimics transfected into them, as seen in Figure 7C. Additionally, PYCR2 levels in LC tissues as well as cells were determined by qPCR analysis. Figures 7D and 7E show that PYCR2 levels were increased in LC tissues as well as cells. Furthermore, miR-338-3p and PYCR2 had an antagonistic relationship in the LC tissues shown in Figure 7F. These results demonstrated that PYCR2 could be regarded as a target of miR-338-3p.

MALAT1 controls the miR-338-3p/PYCR2 axis, which controls the LC cells' ability to proliferate and metastasis

Rescue tests were carried out to further investigate if MALAT1 demonstrated its functional role by controlling the miR-338-3p/PYCR2 pathway. LC cells were first transfected with sh-MALAT1, then with an inhibitor of miR-338-3p and/or sh-PYCR2 (Figure 8A). The outcomes of the CCK-8 and EdU tests then displayed that miR-338-3p inhibitor partially restored the effects of sh-inhibitory MALAT1 on LC cells' ability to proliferate while sh-PYCR2 partially reversed the miR-338-3p inhibitor's boosting mechanism on the LC cells' ability to proliferate (Figures 8B and 8C). Additionally, sh-PYCR2 partially reversed the inhibitory effects of the miR-338-3p inhibitor on the apoptosis of LC cells, while miR-338-3p inhibitor irreversibly altered the promoting effects of sh-MALAT1 on the apoptosis of LC cells in terms of the results of the flow cytometry investigation (Figure 8D). Similarly, information on wound-healing, transwell migration as well as invasion, and the effects of the inhibitors sh-MALAT1 and miR-338-3p on the migration as well as invasion of LC cells all partially reversed. Meanwhile, sh-PYCR2 partial-
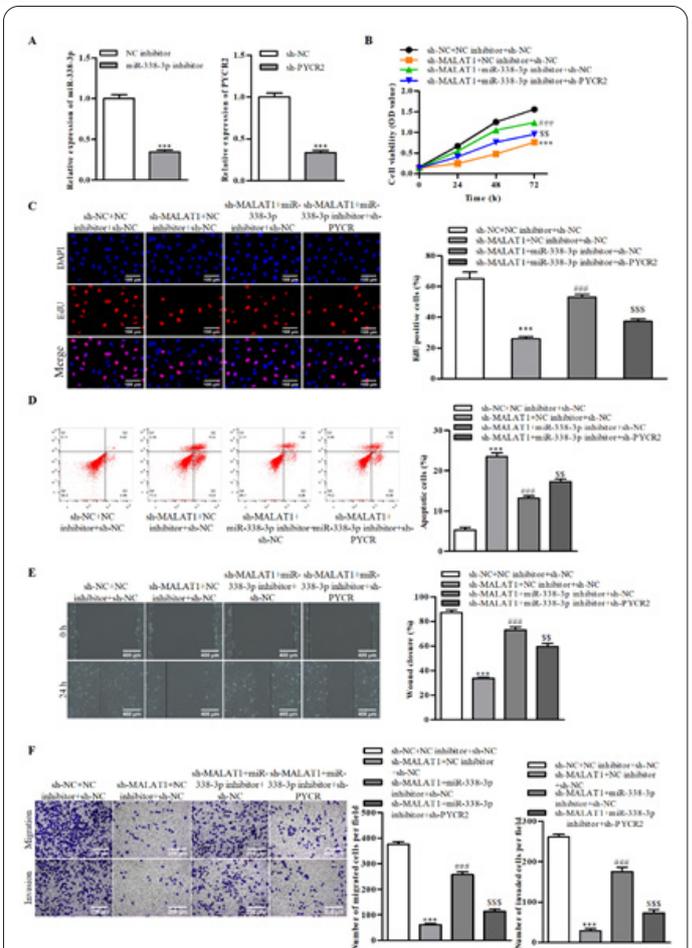
ly reversed their respective promoting effects (Figures 8D to 8F). These findings revealed that MALAT1 controlled the miR-338-3p/PYCR2axis to control the LC cells' ability to proliferate and metastasis.

Discussion

Patients with LC who have metastatic tissues show overexpression of MALAT1. After that, a significant number of research discover that MALAT1 has a crucial impact on the deterioration of LC (18). For instance, Wei *et al.* reveal that the expression of MALAT1 is increased in the tissues as well as cells of NSCLC. Over-expression of MALTA1 promotes NSCLC cell proliferation, motility, migration, and invasion (19). Likewise, MALAT1 is shown to be substantially elevated in serum from NSCLC patients, according to Rong *et al.* By inhibiting cell proliferation, invasion, and death while promoting cell death *in vitro*, MALAT1 knockdown prevents the formation of

tumors (20). MALAT1 levels in NSCLC tissues and cells are also discovered to be abnormally increased by Wang *et al.* MALAT1 inhibition accelerates cell death in vitro while preventing cell proliferation, colony formation, and glycolysis. Additionally, MALAT1 knockdown slows the development of tumors *in vivo* (21). Similar to this, our findings revealed that qPCR and ISH analysis of LC tissues revealed an up-regulation of MALAT1 levels. Lower OS was seen in LC patients with high MALAT1 expressions compared to participants with low MALAT1 levels. MALAT1 expressions were also quite strong in LC cells. Further, LC cell migration, invasion, proliferation, and apoptosis were reduced dramatically by MALAT1 down-regulation utilizing the CCK-8, flow cytometry, EdU, transwell, wound-healing as well as western blot assays. These data suggest that MALAT1 may contribute to the progression and metastasis of LC.

It is widely recognized that lncRNAs may act as ceRNAs to sequester miRNAs in a variety of physiological processes, including LC progression (22). This increases the production of target mRNAs. For instance, human cervical cancer cell lines exhibit markedly increased MALAT1 expression. By adversely influencing miR-429, MALAT1 silencing lowers cervical cell viability, causes cell apoptosis, and suppresses cell invasion potential (23). Likewise, colon cancer tissues as well as cells overexpress MALAT1. By controlling miR-129-5p, MALAT1 inhibition prevents colon cancer from spreading (24). Correspondingly, human prostate cancer tissues as well as cell lines have elevated MALAT1 expression. Through the upregulation of miR-140, MALAT1 knockdown decreases prostate cancer cell's abilities to proliferate, migrate and invade, and promotes cell death (25). Hence, in this research, it was employed online bioinformatics to find miRNAs that interacted with MALAT1. Fortunately, miR-338-3p was picked for more research. On chromosome 17, MiR-338-3p is regarded as a brain-specifically expressed miRNA that has a role in basolateral polarity development and axonal respiration control (26). A recent study broadens the scope of function to include malignancies. MiR-338-3p has been described as a tumor suppressor miRNA because it prevents invasion, migration, and proliferation (27). For instance, tissues and cell lines containing prostate cancer show down-regulation of miR-338-3p. Also, miR-338-3p is forcedly expressed, which inhibits prostate cancer cell's abilities to proliferate, migrate, and invade *in vitro* and tumor formation *in vivo* (28). In addition, colorectal cancer (CRC) cell lines and tissues exhibit reduced miR-338-3p expression levels. Those with low expression of miR-338-3p had significantly lower overall survival (OS) than patients with high expression of miR-338-3p. Up-regulation of miR-338-3p inhibits CRC cells' abilities to proliferate, migrate, and invade as well as colony formation, via inducing apoptosis (29). According to our research, miR-338-3p had a low level of expression in LC tissues as well as cell lines, made a negative correlation with MALAT1, and was associated with LC. Functionally, overexpression of miR-338-3p dramatically decreased LC cells' abilities of viability, proliferating, invading and migrating, as well as induced apoptosis. The partial restoration of the inhibitory effects of MALAT1 deletion on proliferation, apoptosis, and metastasis of LC cells indicates that MALAT1 reduction physically stifled the formation and advancement of LC by manipulating miR-338-3p.

MiRNAs are essential for the development of LC because they control the activity of their downstream target genes (30). In the current work, it was expected that the 3'-UTR of PYCR2 would contain combining sites to miR-338-3p, implying that PYCR2 would be regarded as a target gene for this miRNA. On human chromosome 1q42.12, PYCR2, a key housekeeping protein, decreases 5-pyrroline carboxylic acid (P5C), a substance consisting of glutamic acid as well as ornithine, resulting in proline as well as NAD(P) by its enzymatic reaction (31). There is a growing amount of evidence that PYCR2 is critical for the growth and proliferation of carcinoma cells (32). Taking an instance, it has been observed that PYCR2 is expressed differently in melanoma cells (33,34). PYCR2, a homolog of PYCR2, may also be a novel biomarker for CRC progression and treatment resistance (35). In this study, LC tissues and cells had higher PYCR2 levels, which was in line with the bioinformatic prediction. Additionally, rescue experiments were implemented to thoroughly analyze the MALAT1/miR-338-3p/PYCR2 interactions. PYCR2 inhibition effectively suppressed the miR-338-3p inhibitor's beneficial inotropic actions on the LC cells' abilities to proliferate, apoptosis as well as metastasis which are transfected with sh-MALAT1.

Not to mention, this study demonstrated that MALAT1 was dramatically up-regulated in LC tissues as well as cell lines. Since its knockdown reduced the abilities of viability, proliferating, migrating as well as invading, and caused apoptosis in LC cells applying to control the miR-338-3p/PYCR2 axis, MALAT1 may show to be regarded as a valuable target for lung carcinoma therapy.

Declarations

Conflicts of interest
Yang Geng, Pengfei Chen, Lei Zhang, Xiaojun Li, Chao Song, Xueting Wei, and Huiyuan Gong state that there are no conflicts of interest.

Ethics approval and consent to participate
The experimental protocol was established, according to the ethical guidelines of the Helsinki Declaration and was approved by the Animal Ethics Committee of The First Affiliated Hospital of Bengbu Medical College.

Consent for publication
Not applicable.

Availability of data and material
All data generated or analysed during this study are included in this published article.

Authors' contributions
YG conceived and designed the study. XTW and LZ conducted most of the experiments. XJL analyzed the data. CS performed the literature search and data extraction. PFC drafted the manuscript. YG and HYG finalized

the manuscript. All authors read and approved the final manuscript.

References

1. Toumazis I, Bastani M, Han SS, Plevritis SK. Risk-Based lung cancer screening: A systematic review. Lung Cancer 2020; 147: 154-186.

2. Zhuo C, Zhuang H, Gao X, Triplett PT. Lung cancer incidence in patients with schizophrenia: meta-analysis. Brit J Psychiat 2019; 215(6): 704-711.

3. Zheng M. Classification and Pathology of Lung Cancer. Surg Oncol Clin N Am 2016; 25(3): 447-468.

4. Liam CK, Lee P, Yu CJ, Bai C, Yasufuku K. The diagnosis of lung cancer in the era of interventional pulmonology. Int J Tuberc Lung D 2021; 25(1): 6-15.

5. Oudkerk M, Liu S, Heuvelmans MA, Walter JE, Field JK. Lung cancer LDCT screening and mortality reduction - evidence, pitfalls and future perspectives. Nat Rev Clin Oncol 2021; 18(3): 135-151.

6. Ichikawa T, Hattori A, Suzuki K, et al. Clinicopathological characteristics of lung cancer mimicking organizing pneumonia on computed tomography-a novel radiological entity of pulmonary malignancy. Jpn J Clin Oncol 2016; 46(7): 681-686.

7. Lim ZF, Ma PC. Emerging insights of tumor heterogeneity and drug resistance mechanisms in lung cancer targeted therapy. J Hematol Oncol 2019; 12(1): 134.

8. Zhong S, Golpon H, Zardo P, Borlak J. miRNAs in lung cancer. A systematic review identifies predictive and prognostic miRNA candidates for precision medicine in lung cancer. Transl Res 2021; 230: 164-196.

9. Zhao T, Khadka VS, Deng Y. Identification of lncRNA biomarkers for lung cancer through integrative cross-platform data analyses. Aging (Albany NY) 2020; 12(14): 14506-14527.

10. Chen Z, Lei T, Chen X, et al. Long non-coding RNA in lung cancer. Clin Chim Acta 2020; 504: 190-200.

11. Gong WJ, Yin JY, Li XP, et al. Association of well-characterized lung cancer lncRNA polymorphisms with lung cancer susceptibility and platinum-based chemotherapy response. Tumour Biol 2016; 37(6): 8349-8358.

12. Wang H, Guo M, Ding D, Yang F, Chen Z. Long Non-Coding RNA NNT-AS1 Contributes to Cisplatin Resistance via miR-1236-3p/ATG7 Axis in Lung Cancer Cells. Oncotargets Ther 2020; 13: 3641-3652.

13. Zhang YX, Yuan J, Gao ZM, Zhang ZG. LncRNA TUC338 promotes invasion of lung cancer by activating MAPK pathway. Eur Rev Med Pharmaco 2018; 22(2): 443-449.

14. Zhang N, Jiang W. Long non-coding RNA DANCR promotes HMGA2-mediated invasion in lung adenocarcinoma cells. Oncol Rep 2019; 41(2): 1083-1090.

15. Goyal B, Yadav S, Awasthee N, Gupta S, Kunnumakkara AB, Gupta SC. Diagnostic, prognostic, and therapeutic significance of long non-coding RNA MALAT1 in cancer. Bba-Rev Cancer 2021; 1875(2): 188502.

16. Feng C, Zhao Y, Li Y, Zhang T, Ma Y, Liu Y. LncRNA MALAT1 Promotes Lung Cancer Proliferation and Gefitinib Resistance by Acting as a miR-200a Sponge. Arch Bronconeumol (Engl Ed) 2019; 55(12): 627-633.

17. Gutschner T, Hammerle M, Eissmann M, et al. The noncoding RNA MALAT1 is a critical regulator of the metastasis phenotype of lung cancer cells. Cancer Res 2013; 73(3): 1180-1189.

18. Wang D, Zhang S, Zhao M, Chen F. LncRNA MALAT1 accelerates non-small cell lung cancer progression via regulating miR-185-5p/MDM4 axis. Cancer Med-Us 2020; 9(23): 9138-9149.

19. Wei S, Wang K, Huang X, Zhao Z, Zhao Z. LncRNA MALAT1 contributes to non-small cell lung cancer progression via modulating miR-200a-3p/programmed death-ligand 1 axis. Int J Immunopath Ph 2019; 33: 1681096947.

20. Rong F, Liu L, Zou C, Zeng J, Xu Y. MALAT1 Promotes Cell Tumorigenicity Through Regulating miR-515-5p/EEF2 Axis in Non-Small Cell Lung Cancer. Cancer Manag Res 2020; 12: 7691-7701.

21. Wang S, Wang T, Liu D, Kong H. LncRNA MALAT1 Aggravates the Progression of Non-Small Cell Lung Cancer by Stimulating the Expression of COMMD8 via Targeting miR-613. Cancer Manag Res 2020; 12: 10735-10747.

22. Wang X, Zhang G, Cheng Z, et al. Knockdown of lncRNA ANRIL inhibits the development of cisplatin resistance by upregulating miR-98 in lung cancer cells. Oncol Rep 2020; 44(3): 1025-1036.

23. Shen F, Zheng H, Zhou L, Li W, Xu X. Overexpression of MALAT1 contributes to cervical cancer progression by acting as a sponge of miR-429. J Cell Physiol 2019; 234(7): 11219-11226.

24. Wu Q, Meng WY, Jie Y, Zhao H. LncRNA MALAT1 induces colon cancer development by regulating miR-129-5p/HMGB1 axis. J Cell Physiol 2018; 233(9): 6750-6757.

25. Hao T, Wang Z, Yang J, Zhang Y, Shang Y, Sun J. MALAT1 knockdown inhibits prostate cancer progression by regulating miR-140/BIRC6 axis. Biomed Pharmacother 2020; 123: 109666.

26. Zhang L, Ding F. Hsa_circ_0008945 promoted breast cancer progression by targeting miR-338-3p. Oncotargets Ther 2019; 12: 6577-6589.

27. He J, Wang J, Li S, Li T, Chen K, Zhang S. Hypoxia-inhibited miR-338-3p suppresses breast cancer progression by directly targeting ZEB2. Cancer Sci 2020; 111(10): 3550-3563.

28. Wang Y, Qin H. miR-338-3p targets RAB23 and suppresses tumorigenicity of prostate cancer cells. Am J Cancer Res 2018; 8(12): 2564-2574.

29. Zou T, Duan J, Liang J, et al. miR-338-3p suppresses colorectal cancer proliferation and progression by inhibiting MACC1. Int J Clin Exp Patho 2018; 11(4): 2256-2267.

30. Liu J, Cao L, Zhao N, et al. miR-338-3p inhibits A549 lung cancer cell proliferation and invasion by targeting AKT and beta-catenin signaling pathways. Mol Med Rep 2019; 20(1): 33-40.

31. Afroze B, Mercimek-Andrews S. Pyrroline-5-Carboxylate Reductase 2 Deficiency: A New Case and Review of the Literature. Can J Neurol Sci 2020; 47(2): 280-282.

32. Cai F, Miao Y, Liu C, et al. Pyrroline-5-carboxylate reductase 1 promotes proliferation and inhibits apoptosis in non-small cell lung cancer. Oncol Lett 2018; 15(1): 731-740.

33. Ou R, Zhang X, Cai J, et al. Downregulation of pyrroline-5-carboxylate reductase-2 induces the autophagy of melanoma cells via AMPK/mTOR pathway. Tumour Biol 2016; 37(5): 6485-6491.

34. Kanwal N, Al Samarrai OR, Al-Zaidi HMH, Mirzaei AR, Heidari MJ. Comprehensive analysis of microRNA (miRNA) in cancer cells. Cell Mol Biomed Rep 2023;3 (2): 89-97. doi: Https://doi.org/10.55705/cmbr.2022.364591.1070.

35. Yin F, Huang X, Xuan Y. Pyrroline-5-Carboxylate Reductase-2 Promotes Colorectal Cancer Progression via Activating PI3K/AKT/mTOR Pathway. Dis Markers 2021; 2021: 9950663.